Kinetics and Catalysis, Vol. 43, No. 5, 2002, pp. 677–683. Translated from Kinetika i Kataliz, Vol. 43, No. 5, 2002, pp. 725–732.

Formation of Carbon Filaments from 1,3-Butadiene on Fe/Al_2O_3 Catalysts

V. I. Zaikovskii, V. V. Chesnokov, and R. A. Buyanov

Boreskov Institute of Catalysis, Siberian Division, Russian Academy of Sciences, Novosibirsk, 630090 Russia

Received December 7, 2001

Abstract—The formation of carbon filaments with different crystallographic and morphological characteristics in the course of 1,3-butadiene decomposition on Fe/Al_2O_3 catalysts at low (500–600°C) and high (700–800°C) temperatures was considered in terms of a carbide cycle mechanism. The conditions of formation and decomposition of an iron carbide phase in the course of formation of graphite nanotubes in the low-temperature region were studied.

INTRODUCTION

Undoubtedly, the formation of filamentous carbon in the catalytic decomposition of hydrocarbons on iron-group metals and their alloys with some other metals is of practical importance in addition to scientific interest (as an exotic test material).

The discovery of a carbide cycle mechanism of the formation of carbon filaments [1–3] made it possible to formulate the main ideas and lines of investigation. It was found that the process in general includes the following two stages [3, 4]:

(1) Chemical stage of the catalytic decomposition of hydrocarbons with the formation of carbon atoms;

(2) Physical stage of the formation of graphite crystallization nuclei, the diffusion mass transfer of carbon through a metal particle to the nuclei of crystallization, and the growth of graphite filaments.

Important conclusions on factors that are responsible for the course of the overall process and for the crystallographic and morphological structure peculiarities of carbon deposits can be drawn from this model. These factors are the properties of metal catalyst particles, the nature of the decomposed hydrocarbon, and the process conditions.

Note that the ratio between the rates of the first and second stages, that is, the rates of carbon formation and diffusion transport to a condensation zone in the body of a growing graphite filament, plays a key role. This ratio is responsible for a wide variety of process conditions and specific features in each particular case.

In this work, we chose iron as a test material because the diffusion coefficient of carbon in it is higher than that in the other metals of this group (Ni and Co) by three orders of magnitude. The aim of this work was to study the process by high-resolution electron microscopy depending on the limiting stage: carbide formation, carbide decomposition, or diffusion transfer of carbon through the bulk of iron.

EXPERIMENTAL

The mechanochemical activation of FeOOH and $Al(OH)_3$ powders was used for the preparation of an Fe/Al_2O_3 catalyst [5]. The reduction and carbonization of the catalyst with a composition of 90 wt % Fe_2O_3 and 10 wt % Al_2O_3 were performed in a reactor with the McBain balance. The catalyst was reduced on heating in a hydrogen flow to 550°C for 20–30 min. Alumina was added to stabilize dispersed metal particles by separating them with alumina interlayers.

After the reduction of iron oxide particles to the metal, hydrogen was replaced by argon and the temperature was brought to the specified conditions of carbonization. The carbonization was performed in 1,3-butadiene diluted with argon and hydrogen in the ratio $Ar : H_2 : C_4H_6 = 150 : 40 : 1$ at atmospheric pressure. The dilution with argon was used for excluding harmful side processes of butadiene conversion and for decreasing the rate of carbonization. Hydrogen was added for methanation and the removal of excess carbon from the active surface of catalyst particles (in some cases, an excess of carbon can block the surface).

The carbonization was performed for 120 min; thereafter, the rate of carbon formation decreased at all reaction temperatures. To study the formation of carbon, catalyst samples were also examined at intermediate reaction stages after 5 and 20 min.

The samples were examined on a JEM-2010 high-resolution electron microscope with an accelerating voltage of 200 kV and a line resolution of 0.14 nm. Selected area diffraction and Fourier analysis of high-resolution images were used for phase identification.

RESULTS AND DISCUSSION

Recall that, according to the detailed scheme of the carbide cycle mechanism [1–3], either a metal phase or

0023-1584/02/4305-0677$27.00

Carbon deposition in Fe/Al_2O_3 catalysts carbonized at different temperatures

T, °C	Carbon deposition, wt %	
	20 min	120 min
450	–	6
500	15	75
600	50	280
700	–	460
800	80	490
850	–	150
900	–	20

a carbide phase can be stable depending on process conditions:

$$\mathrm{Fe} \xrightarrow{C_4H_6} |\mathrm{Fe{-}C}| \longrightarrow \mathrm{Fe} + \mathrm{C}$$
$$\mathrm{Fe_3C} \longrightarrow |\mathrm{Fe_3C_{1-x}}|_n + nx\mathrm{C}.$$
$$\mathrm{Fe_3C} \xleftarrow{C_4H_6} |\mathrm{Fe_3C_{1-x}}|_n$$

Here, *n* determines the size of the surface carbide zone that loses one carbon atom, that is, the average surface area responsible for one catalytic center, $nx = 1$; |Fe–C| is a carbide-like intermediate compound; and $|Fe_3C_{1-x}|$ is an intermediate state of carbide with violated stoichiometry.

Previously [6], it was found that the activation energies of carbide formation and decomposition in the course of butadiene decomposition on iron are equal to 89 and 197 kJ/mol, respectively. Thus, at temperatures lower than a critical value (T_{cr}), the rate of carbide formation will be higher than the rate of decomposition and iron will be completely converted into carbide. In the region above T_{cr}, an iron phase will operate. The value of T_{cr} depends on the dispersity of iron and on the nature of the hydrocarbon. According to published data [6], it varied from 670 to 750°C. It was noted that T_{cr} decreased as the catalyst particle size was decreased and as the conditions of the contact of the particles with a graphite phase were improved.

In our experiments, the catalyst after reduction consisted of mixed aggregates of metal particles (α-Fe) and (γ-Al_2O_3). The predominant size of the metal particles was 10 nm, and only a small fraction of the particles was about 100 nm in size. The table summarizes data on the amounts of deposited carbon.

As can be seen, the intense carbonization of the catalyst began at a temperature higher than 500°C, whereas the greatest amount of carbon was formed at 700–800°C. At a temperature higher than 800°C, the amount of deposited carbon decreased, and the samples were almost not carbonized at 900°C.

Based on the concept of the occurrence of the critical temperature T_{cr}, the main measurements were performed within two temperature ranges, 500–600 and 700–800°C.

According to electron-microscopic and electron-microdiffraction data, Fe_3C carbide particles of size 10–100 nm were formed at temperatures of up to 600°C within the first 5 min of reaction. The subsequent carbonization resulted in the formation of carbon filaments as graphite nanostructures and thicker graphite filaments (Fig. 1). Graphite was also detected as layers that covered big catalyst particles.

The thinnest filaments with diameters of 5–20 nm grew most intensely from the outset. In this case, small catalyst particles changed their composition with the appearance of a graphite phase: the carbide decomposed into carbon and α-Fe metal. Metal particles were conically shaped with diameters close to the diameters of filaments.

According to high-resolution electron-microscopic data, carbon filaments of this kind were nanotubes. Their wall thickness was 3–7 nm, and their structure was formed by coaxially conical atomic layers, which resulted from deformation of the (002) planes of the graphite crystal lattice (Fig. 2a). The inclination of the layers to the tube axis varied within an angle range from 0° to 45° in samples prepared at 500°C; however, this range decreased at 600°C, where tubes with graphite layers almost parallel to the axis were predominant (Fig. 2b). The inner channels of filaments occasionally contained partition walls of several graphite monolayers. In our opinion, these partition walls resulted from the detachment of carbon monolayers from the back surface of metal particles at regular intervals as these monolayers were formed in the empty zone of a filament cavity.

The growth of graphite tubes on bigger catalyst particles is of particular interest. At the beginning of the growth, the diameter of these tubes was 30–50 nm; however, it subsequently decreased to 5–20 nm (Fig. 1). In the course of this filament growth, the internal cavity became partially filled with elongated metal particles.

The question arises: how does this happen?

The formation of a stable metal rather than carbide phase at a temperature lower than T_{cr} can be reasonably explained in terms of the carbide cycle mechanism. From the outset, the system goes through a number of stages. Initially, all metal particles are converted into carbide under conditions of hydrocarbon decomposition. As mentioned above, a nonequilibrium carbide phase can be stable for a long time at temperatures lower than 750°C, because the rates of its formation and decomposition are equal. However, even in the early stages of graphite phase formation, conditions favorable for the formation of a thin layer of iron metal occur in a certain zone of the contact of a graphite phase with big catalyst particles (30–50 nm). The equilibrium conditions of the graphite phase at these surface sites of

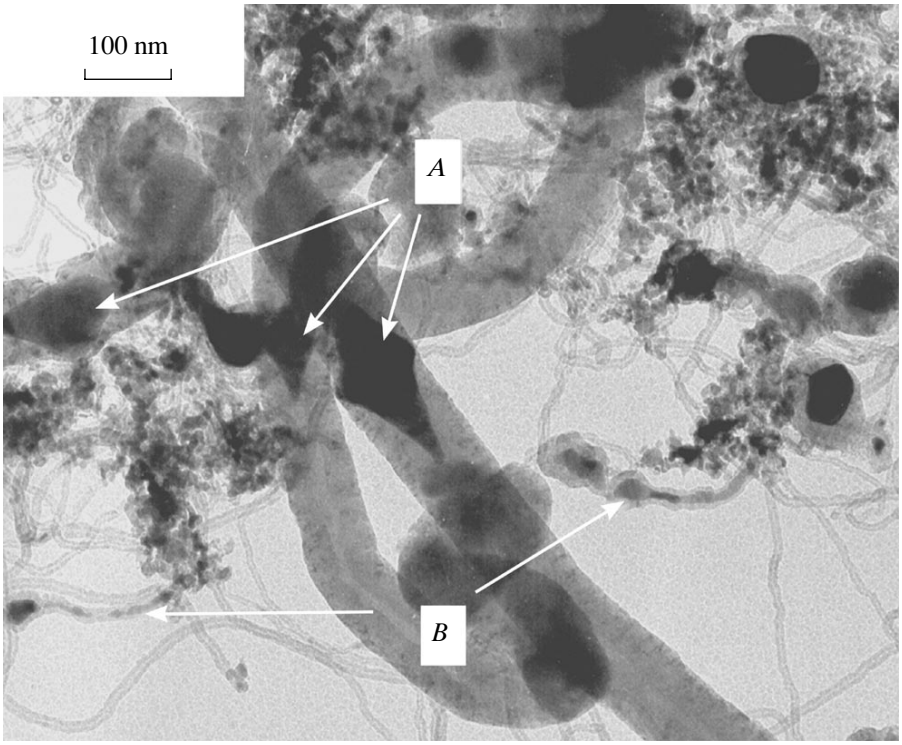

Fig. 1. (*A*) Carbon filaments grown on biconical iron particles and (*B*) nanotubes containing elongated metal particles in the hollow channels of the initial portions of filament growth. The sample was obtained by the carbonization of the Fe/Al_2O_3 catalyst at 500°C for 20 min.

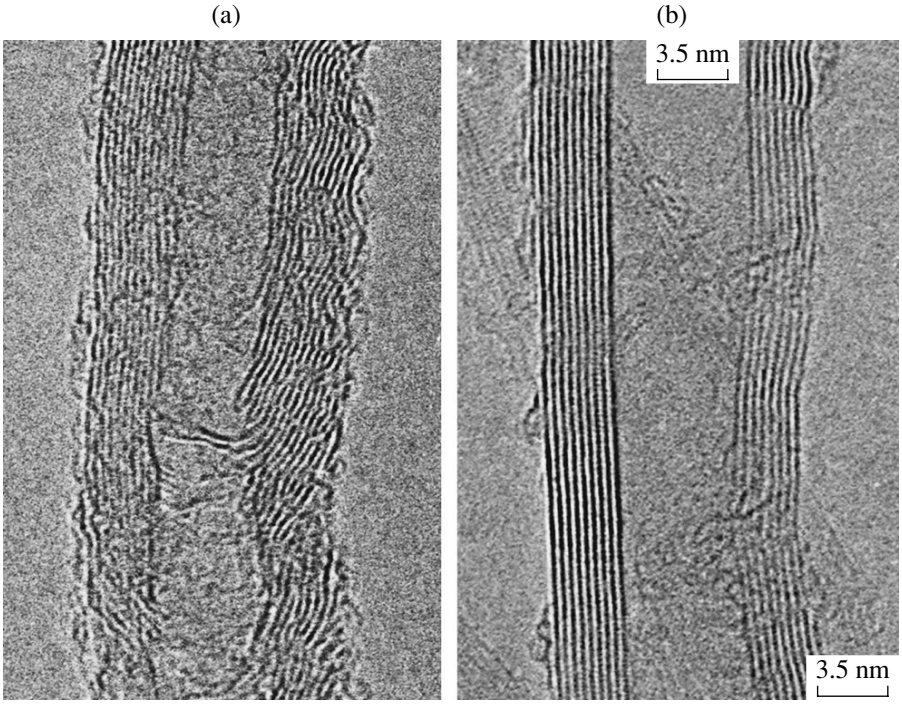

Fig. 2. High-resolution electron micrographs of carbon tubes formed after carbonization at (a) 500 and (b) 800°C for 120 min.

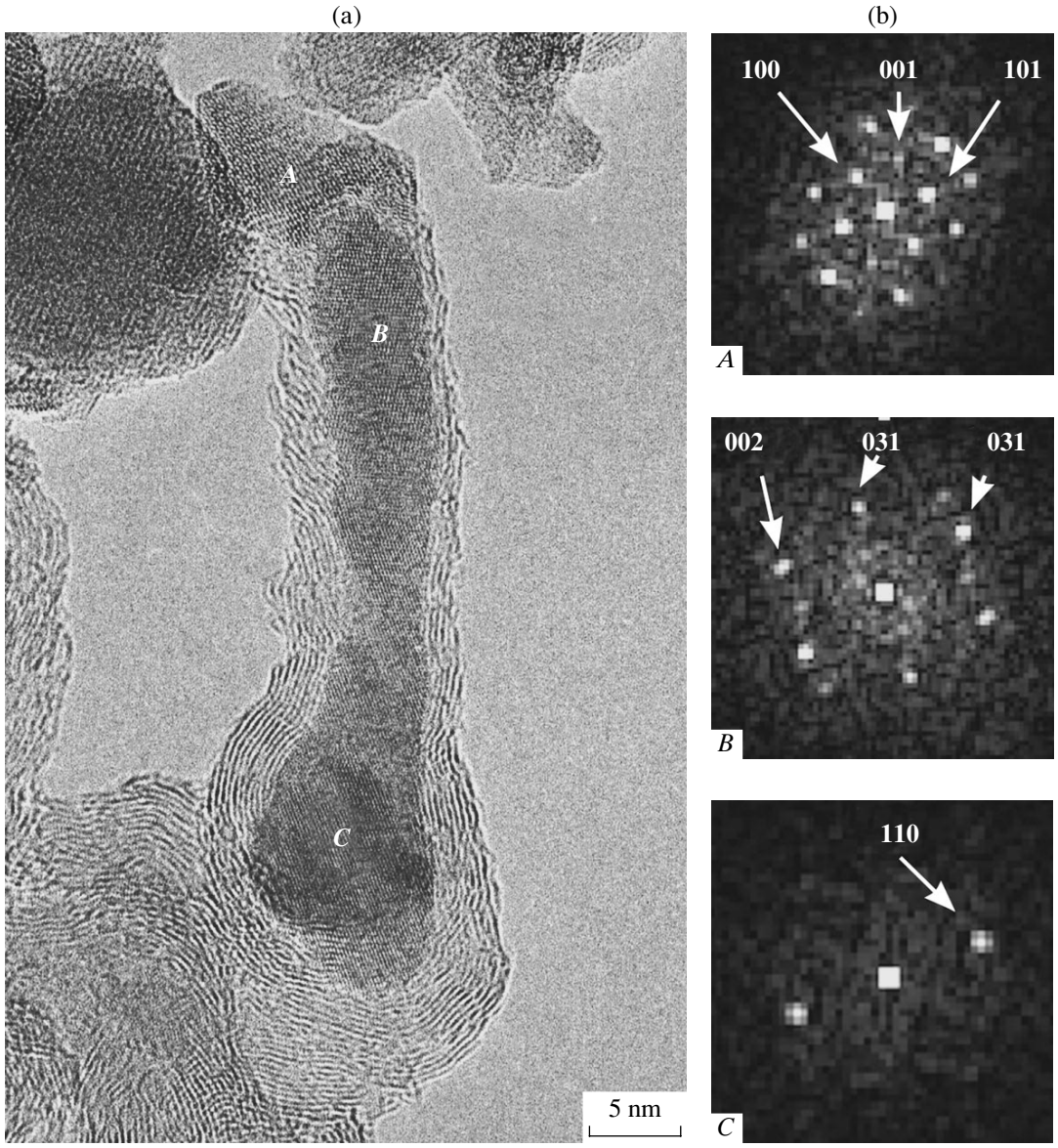

Fig. 3. (a) High-resolution electron micrograph, which demonstrates the elongation of a catalyst particle at the beginning of the growth of a carbon filament at 500°C with separation into the phases of (fragments *A* and *B*) iron carbide and (fragment *C*) iron metal. (b) Fourier transform images of the carbide and metal fragments of a catalyst particle. Arrows indicate reflections with the Miller indices for (fragments *A* and *B*) Fe_3C and (fragment *C*) α-Fe.

a catalyst particle are violated because of the covering with the formed graphite layer; therefore, the reverse conversion into carbide does not occur. At the same time, these processes violate carbide stoichiometry because of carbon formation and activate a carbide particle in the catalytic decomposition of a hydrocarbon. This reaction occurs at a carbon-free part of the particle surface.

The whole of this labile ternary system is subjected to the continuous dynamic migration of carbon atoms through a particle that, at the beginning of reaction, consists of defect carbide and a solid solution of carbon in iron metal. The resulting iron metal in a viscous-flow state is drawn into the free cavity of a graphite filament and separated into fragments. The reason for the appearance of the viscous-flow state in such a system was considered previously [7]. Thus, as a graphite tube grows, the size of its catalytic particle gradually decreases to 5–20 nm. At this size, the prerequisites for the complete conversion of a carbide phase into an iron phase are produced. Correspondingly, a decrease in catalyst particle size results in a decrease in the diameter of graphite tubes. The above consideration is illustrated by Fig. 3, which demonstrates the results of identifying carbide and metal phases, which constitute a catalyst particle elongated within a filament channel.

The above thick filaments with a coaxially conical arrangement of graphite layers inclined to the filament axis by 30°–45° represent the second type of filamentous graphite. In our experiments, these filaments exhibited a constant diameter of 100–150 nm and consisted of two symmetrical branches that grew from the opposite sides of a biconical iron metal particle (Fig. 1). This system, which consists of a biconical metal particle and two symmetrical filaments and appears at a temperature lower than T_{cr}, should be specially considered. This type of carbon deposits is analogous to fibers formed on nickel-containing catalysts. However, it should be noted that, in contrast to the particles of nickel [8] or nickel alloys with copper or palladium [9, 10], a carbide microphase was not formed on the open areas of the surface of biconical iron particles.

Because the diffusion coefficient of carbon through carbide is small and the particle size is considerable, the surface decomposition of the carbide resulted in the almost complete covering of the particle with carbon layers, which prevent the reaction with the hydrocarbon. As a result, the rate of carbide decomposition at these temperatures becomes higher than the rate of carbide formation, and the carbide Fe_3C is converted into the metal. In this case, carbon formed in the bulk of the particle will be released and distributed over the surface of particles in accordance with their morphologies. Nevertheless, filamentous carbon grew on particles with this size. Consequently, the surface of a catalyst particle has sites that are not covered with carbon, and the catalytic decomposition of 1,3-butadiene occurs at these sites in accordance with the growth mechanism of filamentous carbon. The growth of filaments begins simultaneously in two directions, because the particle size is too great to provide the unidirectional diffusion transfer of carbon atoms to the sites of condensation into a graphite phase. As an example, note that we observed the formation of three or four filaments that simultaneously grew from a single particle in the carbonization of nickel–copper alloy particles in methane [11]. In our case, the intense diffusion of carbon through an iron metal particle in two opposite directions resulted in the appearance of an elongated biconical shape, which is symmetric about active surface sites where the catalytic decomposition of 1,3-butadiene took place. In the course of reaction, these sites took the shape of narrow belts (1 to 2 nm wide) located at the periphery of the common base of symmetric cones. The presence of hydrogen in the reaction mixture increased the rate of growth of filamentous carbon because of the removal of a thin carbon film, which deactivates the metal, from the active sites of the particle surface [12]. Because of this, the construction of symmetric graphite filaments continued. However, the bulk diffusion coefficient of carbon in iron is greater than that in Ni or Co by three orders of magnitude. Because of this, the rate of carbon transfer from the narrow periphery band of the common base of cones to the sites of graphite filament growth on the conical surfaces

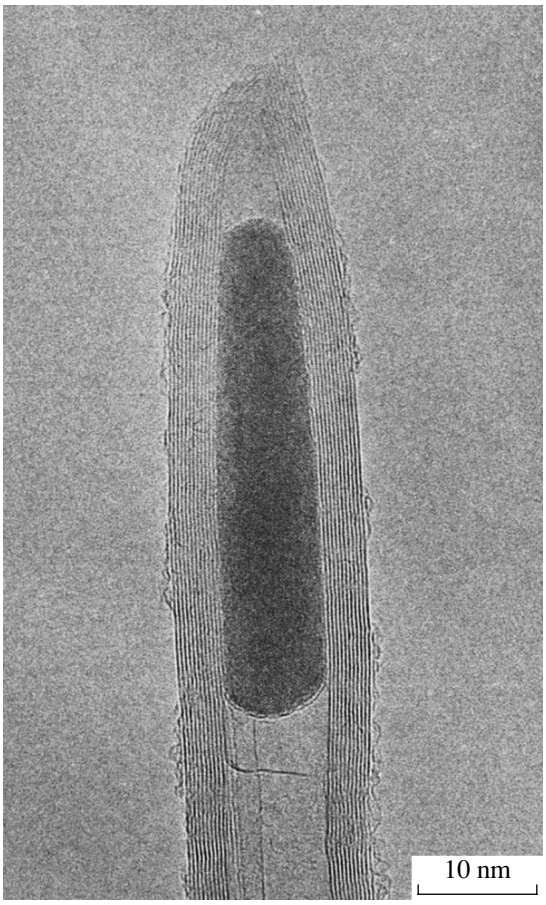

Fig. 4. High-resolution electron micrograph of a metal particle at the end of a nanotube prepared at 800°C.

of particles is greater than the rate of carbide microphase formation [8–10]. This fact explains the absence of the carbide microphase from iron particles in the carbonized Fe/Al_2O_3 catalysts.

Note that the biggest particles about 200 nm in size are significantly covered with graphite layers 5–10 nm in thickness at temperatures lower than 600°C. The great catalyst particle size decreases the role of diffusion in the processes under study to the extent of completely excluding the possibility of filamentous carbon formation. These particles occur in an isolated form and consist of iron metal formed from carbide in the same manner.

Thus, all of the considered cases of the formation of an iron metal phase under conditions of filamentous carbon growth at 500–600°C (below the critical temperature specified in [6]) provide support for the general scheme of a carbide cycle mechanism rather than conflict with the previously formulated concepts.

The results obtained in this study demonstrated that the apparent value of T_{cr} is a complicated function of the ratio between the rates of carbide formation and decomposition. In turn, this ratio depends on the particular conditions of existence of a particle, its size, con-

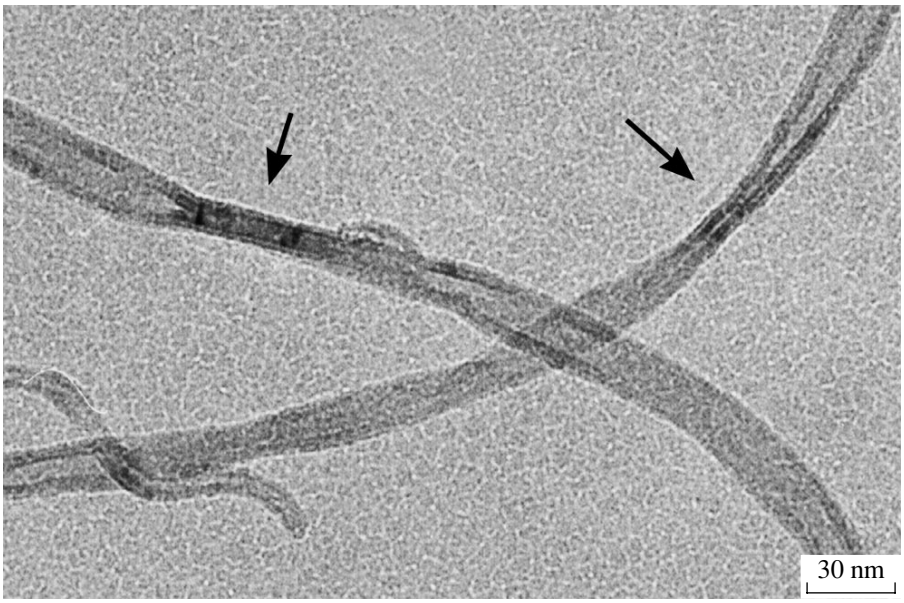

Fig. 5. Carbon nanotubes with flattened regions (marked with arrows).

tact with a graphite phase, the degree of shielding of the particle with graphite layers, the diffusion coefficient of carbon through the bulk of the particle, etc.

At the same time, note that, in all cases when a carbide catalyst particle was converted into a metal particle, the rate of growth of graphite filaments considerably increased. This fact can be explained by the change in the rate-limiting step of the overall process. In the case of carbide, the overall rate of release of atomic carbon is limited by the rate of carbide decomposition. However, at the second physical stage of the process, the diffusion transfer of carbon through the bulk of the particle is required for the construction of a graphite filament. The diffusion coefficient of carbon through the carbide Fe_3C is lower than that in a solid solution of iron by several orders of magnitude [13]. Because of this, the growth of a graphite phase on carbide is extremely slow, and the particles are strongly shielded by graphite layers. In iron particles, the diffusion transfer of carbon does not limit the construction of a graphite filament, and the contact of the particles with carbon only accelerates the removal of carbon from the carbide.

In conclusion, let us consider the formation of carbon filaments as graphite tubes in the temperature range 700–800°C, that is, certainly higher than the critical temperature.

In this range, the rate of carbide decomposition is knowingly higher than the rate of carbide formation, and particles of any size were retained as iron metal from the outset. The chemical stage, that is, the catalytic decomposition of the hydrocarbon, was a rate-limiting step in the filament growth. The process occurred at the highest rates and with the greatest yields of carbon (see the table). The resulting samples were reasonably homogeneous with respect to the morphology of carbon. High diffusion coefficients at these temperatures resulted in the formation of only a single form of thin carbon filaments (nanotubes) 5–20 nm in diameter and up to tens of micrometers in length. According to high-resolution electron-microscopic data, the structure of nanotube walls is formed from two to ten coaxially cylindrical graphite monolayers (Fig. 2b). The nanotubes grew because of highly dispersed metal particles located at their ends.

Big metal particles, which were present in the initial reduced state of the catalyst, also participated in the growth of nanotubes. Under reaction conditions at the specified temperature, the metal became highly fluid, and it was distributed over a hollow channel to decrease the diameter of the growing filament. The further growth of the nanotube took place at a highly dispersed metal particle, which was separated from a spread big particle. It is likely that, under the reaction conditions, the surface of a small active metal particle located at the end of a graphite nanotube was in contact with the ends of cylindrical graphite layers. This structure of metal–graphite interfaces was found previously [8] in the growth of graphite tubes on nickel particles. The electron micrographs of samples demonstrated that the termination of reaction resulted in the disappearance of the active state of an iron metal particle, its inclusion into a filament channel, and encapsulation with free graphite layers (Fig. 4).

In this temperature range, the shapes of the thinnest graphite tubes were distorted because of flattening up to the complete closure of the walls. This resulted in the formation of tube portions as flat graphite bands (Fig. 5). The flattening was observed at the sites where

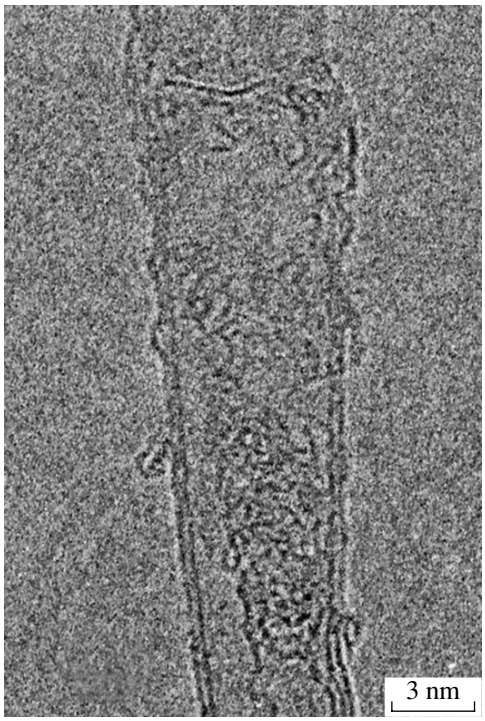

Fig. 6. High-resolution electron micrograph of a nanotube region with amorphous carbon inside and outside the tube.

the thin layers of amorphous carbon were deposited on the walls of the tubes on both the outside and the inside (Fig. 6). The mechanism of the high-temperature formation of amorphous carbon is beyond the scope of this paper. Although the amount of amorphous carbon was small, it had a strong effect on the morphology of the nanotubes; as noted, it distorted their cylindrical shape up to the closure of the nanotube walls.

This phenomenon is related to a problem of nanotube construction energetics that is of fundamental importance. As the tube diameter decreased, the degree of curvature of graphite planes closed as cylinders increased and the energy of deformation correspondingly increased [14]. The internal and external diameters of these tubes are small and fall within the limits of 5–20 nm. The energy of deformation of these tubes is as high as 50 kJ/mol. It is likely that the contact of amorphous carbon with the walls of the graphite tubes resulted in the reaction of amorphous carbon with structurally organized cylindrical graphite layers, in the weakening of the bonds of carbon atoms in the graphite structure, and in the relaxation of the stored energy of deformation on the straightening of the cylindrical layers.

Finally, note that an increase in the temperature up to 850–900°C resulted in the impossibility of formation of carbide compounds and in the shielding of metal particles with a pyrocarbon film.

ACKNOWLEDGMENTS

This work was supported by the Russian Foundation for Basic Research (project nos. 99-03-32420 and 00-03-32431) and the Program “Leading Scientific Schools of Russia” (grant no. 00-15-7440).

REFERENCES

1. Buyanov, R.A., Chesnokov, V.V., Afanas’ev, A.D., and Babenko, V.S., *Kinet. Katal.*, 1977, vol. 18, no. 4, p. 1021.
2. Buyanov, R.A., Chesnokov, V.V., and Afanas’ev, A.D., *Kinet. Katal.*, 1979, vol. 20, no. 1, p. 207.
3. Buyanov, R.A., *Zakoksovanie katalizatorov* (Catalyst Coking), Novosibirsk: Nauka, 1983.
4. Buyanov, R.A. and Chesnokov, V.V., *Zh. Prikl. Khim.*, 1979, vol. 70, no. 6, p. 978.
5. Avvakumov, E.G., *Mekhanicheskie metody aktivatsii khimicheskikh protsessov* (Mechanical Methods of Activating Chemical Processes), Novosibirsk: Nauka, 1986.
6. Chesnokov, V.V., Buyanov, R.A., and Afanas’ev, A.D., *Kinet. Katal.*, 1979, vol. 20, no. 2, p. 477.
7. Buyanov, R.A. and Chesnokov, V.V., *Khim. Interes. Ust. Razv.*, 1995, vol. 3, no. 3, p. 177.
8. Zaikovskii, V.I., Chesnokov, V.V., and Buyanov, R.A., *Kinet. Katal.*, 2001, vol. 42, no. 6, p. 890.
9. Zaikovskii, V.I., Chesnokov, V.V., and Buyanov, R.A., *Kinet. Katal.*, 1999, vol. 40, no. 4, p. 612.
10. Zaikovskii, V.I., Chesnokov, V.V., and Buyanov, R.A., *Kinet. Katal.*, 2000, vol. 41, no. 4, p. 538.
11. Chesnokov, V.V., Zaikovskii, V.I., Buyanov, R.A., *et al.*, *Catal. Today*, 1995, vol. 24, no. 24, p. 265.
12. Chesnokov, V.V. and Buyanov, R.A., *Usp. Khim.*, 2000, vol. 69, no. 7, p. 675.
13. Osturk, D., Fearing, V.Z., Ruth, J.J., and Simkovich, G., *Metall. Trans. A*, 1982, vol. 13, p. 1871.
14. Tibbets, G.G., *J. Cryst. Growth*, 1984, vol. 66, p. 632.